



Molecular Docking of Ferulic Acid Derivatives on P2Y₁₂ Receptor and their ADMET Prediction

Juni Ekowati¹, Nuzul Wahyuning Diah¹, Kholis Amalia Nofianti¹,
Iwan Sahrial Hamid² & Siswandono¹

¹Department of Pharmaceutical Chemistry, Faculty of Pharmacy,
Kampus B Universitas Airlangga, Jalan Airlangga No. 4-6,
Surabaya 60115, Jawa Timur, Indonesia

²Department of Basic Veterinary Medicine, Faculty of Veterinary Medicine,
Kampus C Universitas Airlangga, Jalan Dr. Ir. H. Soekarno, Mulyorejo,
Surabaya 60115, Jawa Timur, Indonesia
E-mail: j_ekowati@yahoo.com

Abstract. P2Y₁₂ is a platelet receptor that is involved in ADP signal transduction and is an attractive target for antithrombotic drugs. The side effects of antithrombotic drugs are not pleasant for the patient, so research into the development of new antithrombotic agents is still necessary. Evaluation of absorption, distribution, metabolism, elimination, and the toxicity profile of candidate drugs is an important step in drug development. The aim of this study was to predict the potency of ferulic acid (FA) and its derivatives (FA1-24) as antiplatelet drugs by a docking study on the P2Y₁₂ receptor (PDB ID: 4PXZ) and their ADMET performance. The docking study was performed using Molegro Virtual Docker, version 5.5. ADMET prediction of FA was conducted using the pkCSM online tool. The results of the *in silico* study showed that FA-19 had the lowest MolDock score (MDS), which means that this compound is predicted to have the greatest activity. FA-19 is also predicted to be practically non-toxic. It is expected that FA-19 will have good intestinal absorption and is similarly distributed in the intestine and in the blood plasma. Its penetration in the blood-brain barrier is moderate but does not inhibit the CYP2D6 and CYP3A4 enzymes.

Keywords: ADMET prediction; antiplatelet; ferulic acid; molecular docking, P2Y₁₂ receptor.

1 Introduction

Cardiovascular diseases and strokes are major problems of morbidity and mortality in many countries, including Indonesia. In Indonesia, the prevalence of heart and blood vessel diseases continuously increases and the prevalence of coronary heart disease (CHD) in 2013 was 0.5%. Deaths caused by cardiovascular diseases, especially CHD and strokes, are predicted to increase up to 23.3 million by 2030 [1].

P2Y₁₂ receptors play an important role in thrombus formation, i.e. in ADP signal transduction, and are an attractive target for antithrombotic drugs such as Prasugrel and Cangrelor [2-4]. The P2Y₁₂ receptor can be used as a therapeutic target and can be applied to molecular modeling and structure-activity relationship based drug design [5]. Unfortunately, the current antithrombotic drugs possess undesired side effects, such as bleeding and hemostasis problems. Therefore, research on drug design of new antiplatelet agents is important [6].

Drug design is an attempt to improve existing drugs or compounds with specific pharmacological activity and is often described as a systematic elaboration process with the aim of obtaining new drugs with better activity and reducing any side effects that exist through molecular manipulation. The structural changes of a compound will alter the physicochemical properties of the compound, including its lipophilic, electronic and steric properties, which may cause changes in its biological activity [7,8].

One of the cinnamic acid derivatives, i.e. (*E*)-3-(4-hydroxy-2-methoxyphenyl) propenoic acid or ferulic acid (FA3), has been reported as an inhibitor of platelet aggregation through *in vitro* assay [9]. The mechanisms of ferulic acid in preventing platelet aggregation are: (1) inhibiting the [Ca²⁺] channel on the cell membrane surface and interfering with phospholipase C in releasing [Ca²⁺] to reduce the combination of ADP with P2Y₁₂; and (2) inhibiting the synthesis of TXA₂, which can bind to TXA₂R to activate platelets [10]. In an effort to obtain an effective and safe anti-platelet compound, an *in silico* assay of FA derivatives (FA1-24) was observed through a docking study on the P2Y₁₂ receptor (PDB ID: 4PXZ).

An *in silico* assay is conducted by docking a molecule to predict its activity with the selected target cell. Docking is an attempt to harmonize the ligand, a small molecule inside the target cell, which is a large protein molecule [11]. The results of the *in silico* test are in the form of bond energy values, or the Moldock score (MDS). The bond energy indicates the amount of energy required to form a bond between the ligand and the receptor. The lower the bonding energy, the more stable the bond. If the ligand bond with the receptor is stable, it can be predicted that the activity will be stronger [12].

Besides measuring docking activity, one of the principle stages in drug design is the evaluation of the pharmacokinetic properties, i.e. the absorption, distribution, metabolism, elimination, and toxicity (ADMET), of the candidate drug [13]. ADMET analysis using an animal model is expensive, so we used molecular modeling in an effort to predict the chemical properties of the molecular chemistry, the pharmacokinetic properties (ADME), and the toxicity of the compounds [13,14].

2 Material and Method

2.1 Receptor

The molecular structure of P2Y₁₂ receptors can be downloaded via a protein data bank site [15]. The P2Y₁₂ receptor with PDB ID: 4PXZ was selected, which contains a ligand (5-(6-amino-2-(methylthio)-9H-purine-9-yl) -3,4-dihydroxyte - trahydrofuran-2-yl)-methyl diphosphate code 6AD_1201[A].

2.2 Ligand

The structure of the ligands (FA1-24) was drawn using the 2D/3D ChemBio Draw Ultra software application, version 12 (Cambridge Soft) and then copied into the ChemBio 3D Ultra software application, version 12, to create the 3D structure and measure its minimum energy using MMFF94. This was then stored as mol2 {SYBYL2 (*.Mol2)}.

2.3 Validation of Docking Study

The validation of the docking study was performed by re-docking the ligand reference into an appropriate protein cavity. Re-docking is accepted if the root mean square value (RMSD) < 2.0 Å°.

2.4 Docking Study

The docking study of these compounds on the P2Y₁₂ receptor (4PXZ) was conducted using Molegro Virtual Docker, version 5.5. (Molegro ApS). The best docking results can be detected visually by comparing the structure of the docked molecules with the crystal structure of the reference ligand (6AD_1202 [A]) in the binding site. The results are presented as MolDock scores (Figure 1). The lowest energy indicates the best binding pose between the functional group of the ligand and the amino acid residue of the protein. The ligand-protein complexes with the lowest MDS were used for further visual examination (Figures 2-6).

2.5 Prediction of ADME and Toxicity of Compounds

Prediction of the pharmacokinetic properties (ADME: absorption, distribution, metabolism, and excretion) and toxicity of the FA derivatives was performed using the pkCSM online tool, i.e. firstly the tested compounds and the comparative compound were drawn as 2D molecular structures with ChemBio Draw Ultra and copied into ChemBio 3D Ultra to create a 3D structure, and then stored as *.sdf file or *.pdb files. Secondly, all of the tested compounds and the comparative compound were translated into SMILES format using SMILES Translator Online Help [16]. In the SMILES format, the compounds

were processed using the pkCSM online tool [17] to predict the ADME and the toxicity of the compounds. Also, the ProTox online tool [18] was used to predict oral rodent toxicity by determining the LD50 value and the classification of compound toxicity based on the Globally Harmonized System (GSH).

3 Results and Discussion

3.1 Docking Study

Molecular docking was carried out to elevate and develop the pharmacological activity of the FA derivatives. To explain the mode of binding between the FA derivatives and human P2Y₁₂ receptor, docking studies were performed using the X-ray crystal structure of human P2Y₁₂ in complex with its full agonist onto PDB ID: 4PXZ.

The MolDock score is a differential evolution algorithm in the Molegro Virtual Docker program. The MDS, or E_{score} , is the sum of E_{inter} and E_{intra} by Eq. (1), E_{inter} is estimated by Eq. (2) and E_{intra} is estimated by Eq. (3).

$$E_{score} = E_{inter} + E_{intra} \quad (1)$$

$$E_{inter} = \sum_{i=ligand} \sum_{j=protein} \left[E_{PLP}(r_{ij}) + 332.0 \frac{q_i q_j}{4r_{ij}^2} \right] \quad (2)$$

$$E_{intra} = \sum_{i=ligand} \sum_{j=protein} [E_{PLP}(r_{ij})] + \sum_{flexible\ bond} A [1 - \cos(m\theta - \theta_o)] + E_{clash} \quad (3)$$

E_{inter} is the ligand-receptor interaction energy, while E_{intra} is the internal energy of the ligand. E_{PLP} is calculated by two different parameters, i.e. the van der Waals interaction and the electrostatic interactions [19].

The MDS of the FA derivatives (FA1-24) can be seen in Figure 1. The MDS of the reference ligand (5-(6-amino-2-(methylthio)-9H-purine-9-yl)-3,4-dihydroxytetrahydrofuran-2-yl)-methyldiphosphate, code 6AD_1202[A] is -187.880 kcal/mol, while its RMSD value is 1.87 Å.

Based on the data presented in Figure 1, all FA derivatives (FA4-24) apart from FA1 and FA2 have an MDS value lower than FA3 (ferulic acid), as is generally known. The structure modification of FA3 to FA2 through the demethylation of the methoxy moiety of FA3 to the hydroxyl moiety of FA2 decreased the molar refractivity (MR) and the MDS. The structure modification of FA3 to FA1 through hydrogenation of the vinylic double bond of FA3 also decreased the MDS. Therefore, it is concluded that the methoxy and the vinylic double bond are important moieties interacting with the P2Y₁₂ receptor.

Structure modification of the phenolic group of FA3 with the benzoyl- and substituted-benzoyl moieties (FA16-19) leads to different three-dimensional (3D) shapes of the compounds, so their interactions with the receptor are more effective, especially the steric interactions. Molecule FA19 ((E)-3-(3-methoxy-4-((4-methoxybenzoyl)oxy)phenyl)acrylic acid) had the lowest MDS, i.e. -159.804 kcal/mol, while molecule FA3 had MDS -111.140 kcal/mol.

Compound FA19 had the highest PSA (A2) value (Table 2) among the other derivatives, enabling greater receptor interaction. Therefore, it can be predicted that the bond between molecule FA19 and the P2Y₁₂ receptor as the target protein is more stable than for FA3. This bond is the strongest among the other derivatives.

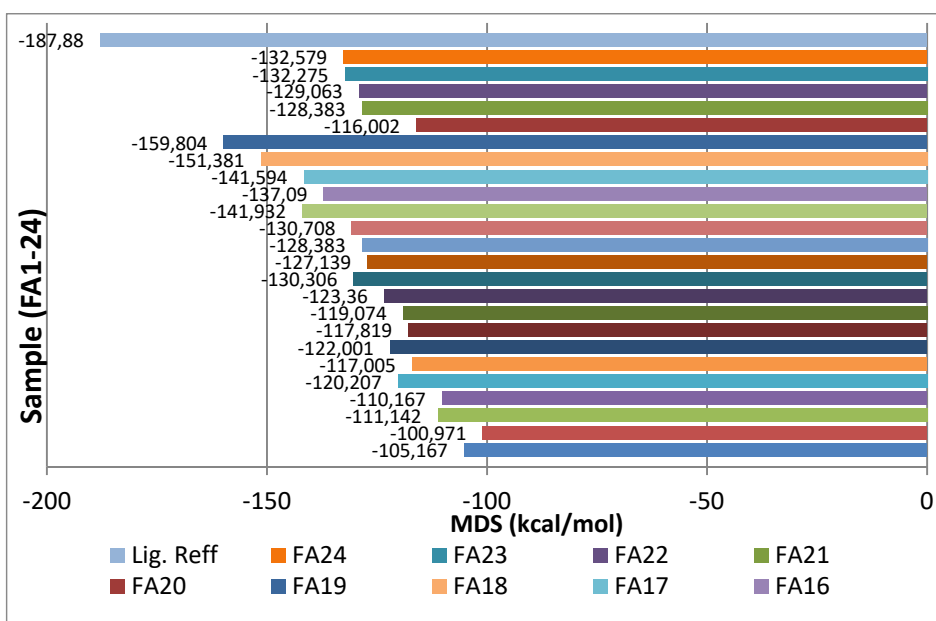


Figure 1 Barchart of the MolDock Score (MDS) of FA derivatives (FA1-24) by Molegro Virtual Docker. PDB ID: 4PXZ (x = MDS; y = sample).

The P2Y₁₂ receptor responds to the ADP signal and participates in the inhibition of adenylyl cyclase, Ca²⁺-dependent cell migration, regulation of cell morphology, and cellular aggregation. P2Y₁₂ must be stimulated for ADP-induced platelet aggregation to occur, which can be prevented by a substance that impartially inhibits the receptor. P2Y₁₂ has a specific tissue distribution, making it an important target for therapeutic intervention [2] so that the compound binding to the receptor will inhibit P2Y₁₂ activity in platelet

aggregation. The best docking position in the 3D structure molecules of 6AD_1201[A]-FA3-FA19 can be seen in Figure. 2.

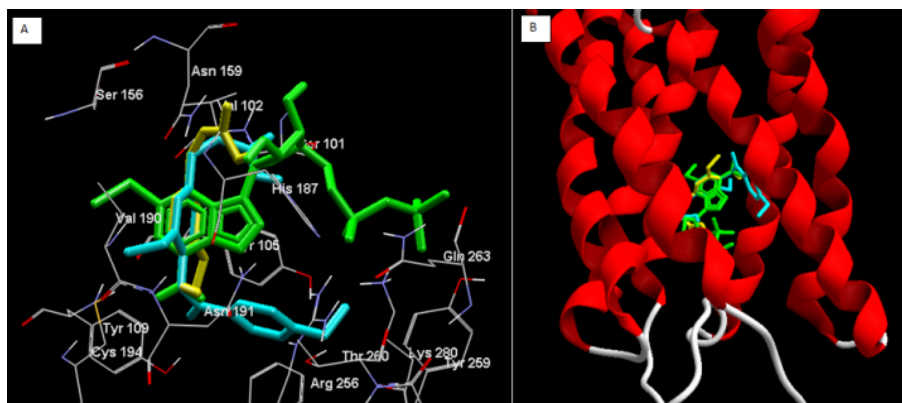


Figure 2 The binding mode of compound 6AD_1201[A], FA3 and FA19 to the P2Y₁₂ receptor. (A) The best docking position of the 3D structures of 6AD_1201[A] (green), FA3 (yellow), FA19 (blue) in stick style; residue amino acids are shown as lines and ligands are represented by thick lines with a fixed color. (B) The best docking position of 6AD_1201[A] (green), FA3 (yellow), FA19 (blue) with P2Y₁₂ represented as a red ribbon.

The docking study was carried out at cavity 2; Vol. 74.752; surface: 264.56. The interactions of each molecule, i.e. 6AD_1201[A], FA3 and FA19, are displayed in Figures 3-5.

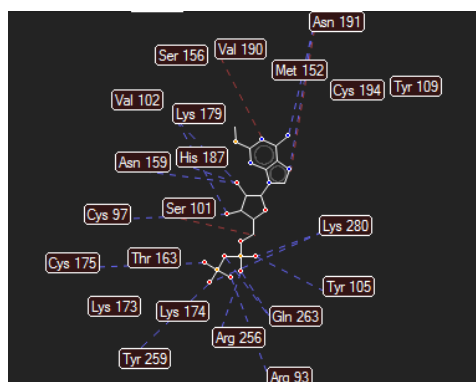


Figure 3 The interaction of the functional groups of molecule 6AD_1201[A] with the P2Y₁₂ receptor (PDB ID: 4PXZ) in 2D form. The blue line represents the hydrogen bonding interaction and the red line represents the steric interaction.

In Figure 3, the interaction between molecule 6AD_1201[A] and the P2Y₁₂ receptor can be seen. Hydrogen bonding interaction occurs between the

phosphate groups of molecule 6AD_1201[A] and the amino acid residues, i.e. Arg93, Cys97, Ser101, Tyr105, Thr163, Cys175, His187, Lys280, Arg256, Tyr259. In addition, steric interactions of the adenosine moiety take place with the residues Asn191 and Val190.

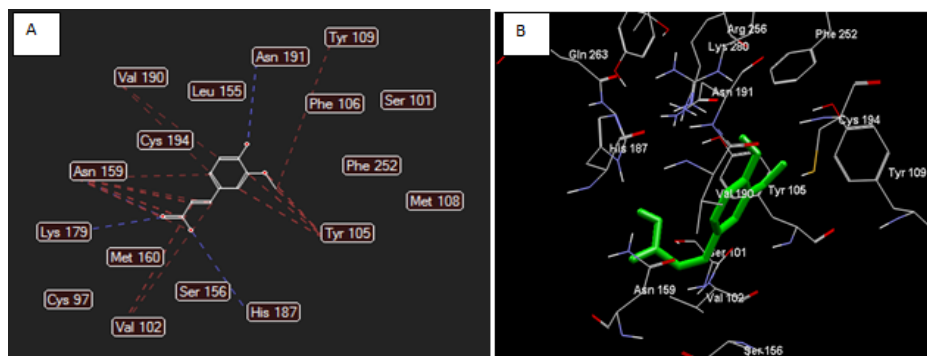


Figure 4 Interaction of the functional groups of molecule FA3 with the P2Y₁₂ receptor (PDB ID: 4PXZ) in 2D form (A) and 3D form (B). The blue line represents the hydrogen bonding interaction and the red line represents the steric interaction. The residue amino acids are shown as thin lines and the ligand is shown as a thick line with a fixed color.

According to Figure 4, the molecule FA3 compound has three hydrogen bonds with Hys187, Lys179, Ser156, Asn191 and Cys194. In addition, FA3 also has steric interaction with amino acid residues of the P2Y₁₂ receptor, i.e. Val102, Tyr105, Tyr109, Ser156, Asn159, Val190.

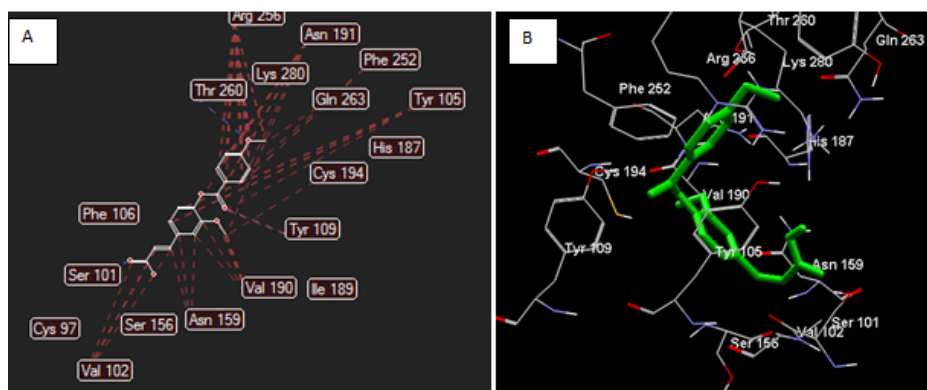


Figure 5 The interaction of the functional groups of molecule FA19 with the P2Y₁₂ receptor (PDB ID: 4PXZ) in 2D form (A) and 3D form (B). The residue amino acids are shown as thin lines and the ligand is shown as a thick line with a fixed color. The blue lines represent hydrogen bonding interaction and red lines represent steric interactions.

Based on Figure 5, there was a modification in the phenolic moiety of FA3 into the *p*-methoxybenzoyl moiety of FA19. This modification led to an increase of the interaction between the FA19 molecule and the amino acid residues in the P2Y₁₂ receptor. The carboxylate group of FA19 molecules has hydrogen bonds with the residues Val102, Ser101, and Phe106. In addition, the methoxy group possesses hydrogen bonds with residue Thr260. The *p*-methoxybenzoyloxy-moiety of FA19 has hydrogen bonding with Tyr109. The FA19 molecule has steric interaction with Tyr105, Ser156, Leu154, Pro158, Asn159, Trp186, Val190, Asn191, and Arg256 residues of the P2Y₁₂ receptor. Besides hydrogen bonding interaction, the *p*-methoxybenzoyl-moiety of FA19 also contributes to hydrophobic interaction with Asn191, Tyr105, and Arg256, thus enhancing the interaction with that receptor.

These docking studies suggest that FA3 and FA19 have a distinct binding pose with 6AD_1201[A] as ligand reference, except Tyr105, Val190 and Arg256. The P2Y₁₂ receptor antagonist, i.e. 2-MeSADP, has hydrophobic interactions with the Tyr105, Val190, and Leu155 residues, i.e. the same as FA3 and FA19 [2].

3.2 ADMET Profiles

Chemical databases contain hundreds of thousands of molecules that could be suitable ligands for a receptor. But, no matter how good the fit with the receptor, the candidate molecule is of no use if the absorption is poor or if the drug is excreted too slowly from the body. 2245 drugs from the World Drugs Index database were analyzed and it was concluded that a compound is more likely to have poor absorption or permeability if: the molecular weight exceeds 500; the calculated octanol/water partition coefficient (log P) exceeds +5; there are more than 5 H-bond donors (HBD) expressed as the sum of O–H and N–H groups; and there are more than 10 H-bond acceptors (HBA) expressed as the sum of N and O atoms. The above analysis is called the Lipinski Rules of Five because all values are multiples of five [20].

The results of the *in silico* study of the physicochemical properties of the FA derivatives can be seen in Table 1. Based on Table 1, it can be seen that the molecular weight values of the ferulic acid derivatives (FA1-24) ranged from 180.159 to 332.739 (<500), the value of log of the octanol/water partition coefficient (log P) ranged from 1.20 to 3.67 (< 5), the amount of HBD ranged from 3 to 5 (≤ 5), and the amount of HBA ranged from 1 to 3 (< 10). This means that all derivatives meet the Lipinski Rules of Five [20]. Hence, it can be predicted that these FA derivative compounds will be easily absorbed and have high permeability.

Table 1 Prediction of *In Silico* values of physicochemical properties of ferulic acid derivative compounds using pkCSM Online Tool.

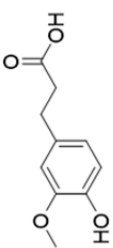
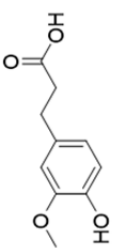
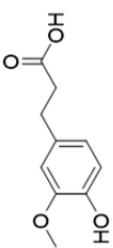
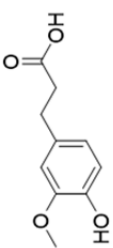
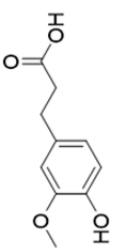
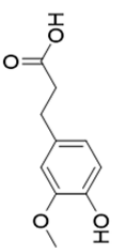
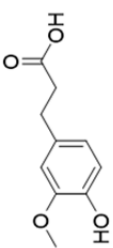
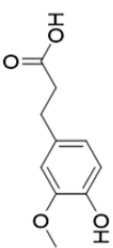
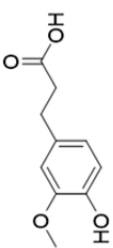
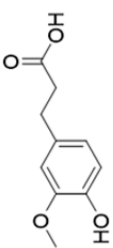
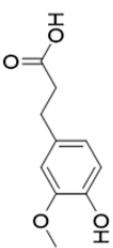
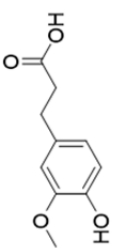
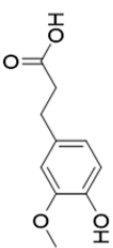
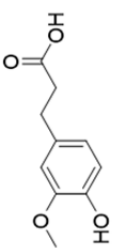
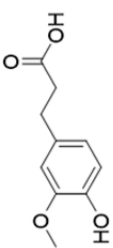
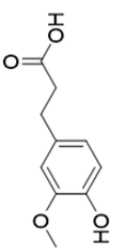
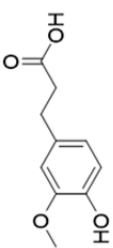
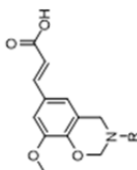
Code	R ₁	R ₂	R ₃	MW	Log P	Torsion	Etotal	MR	HBA	HBD	PSA (Å ²)	Water solubility
FA1				196.202	1.42	4	5.0809	50.06	3	1	81.755	-1.534
FA2			H	180.159	1.20	2	3.6938	46.48	3	3	74.381	-1.223
FA3			CH ₃	194.186	1.50	3	16.3588	51.92	3	2	81.065	-1.603
FA4			CH ₃	208.213	1.59	3	24.3828	57.35	4	1	87.749	-1.690
FA5			C ₂ H ₅	222.240	1.98	4	24.6997	60.75	4	1	94.114	-2.038
FA6			C ₃ H ₇	236.267	2.37	5	25.3019	66.75	4	1	100.479	-2.523
FA7			C ₄ H ₉	250.294	2.76	6	25.9635	71.35	4	1	106.844	-3.020
FA8			C ₃ H ₁₁	264.321	3.15	7	26.7322	75.95	4	1	113.209	-3.519
FA9			CH ₃	222.240	1.89	4	32.5638	62.79	4	1	94.434	-2.263
FA10			CH ₃	236.223	1.72	4	15.9918	61.31	4	1	98.276	-2.166
FA11			COCH ₃	264.233	1.64	4	18.8092	65.26	5	1	108.80	-2.354
FA12			CH ₃	250.250	2.11	5	16.5332	66.05	4	1	104.641	-2.573
FA13			CH ₃	264.277	2.50	6	30.2531	70.65	4	1	111.006	-2.993
FA14			CH ₃	278.304	2.89	7	31.7653	75.25	4	1	117.371	-3.419
FA15			CH ₃	292.331	3.28	8	32.4769	79.85	4	1	123.736	-3.842
FA16			CH ₃	298.294	3.01	5	20.2020	81.43	4	1	126.968	-4.122
FA17			CH ₃	332.739	3.67	5	20.9919	86.04	4	1	137.271	-4.776

Table 1 (cont.) Prediction of *In Silico* values of physicochemical properties of ferulic acid derivative compounds using pkCSM Online Tool.

Code	R ₁	R ₂	R ₃	MW	Log P	Torsion	Etotal	MR	HBA	HBD	PSA (Å ²)	Water solubility
FA18	COC ₆ H ₅ (4-CH ₃)	H	CH ₃	312.321	3.32	5	31.9885	87.33	4	1	133.333	-4.393
FA19	COC ₆ H ₅ (4-OCH ₃)	H	CH ₃	328.320	3.02	6	40.1577	88.68	5	1	138.446	-4.271
FA20				249.266	1.58	3	13.4521	70.19	4	1	105.233	-1.924
FA21				263.293	1.96	4	17.2710	74.99	4	1	111.600	-2.182
FA22				277.320	2.35	5	15.5845	79.59	4	1	117.963	-2.557
FA23				311.337	3.15	4	19.6146	89.36	4	1	133.925	-4.432
FA24				325.364	3.46	4	21.2404	95.26	4	1	140.290	-4.697



R = CH₃

R = C₂H₅

R = C₃H₇

R = C₆H₅

R = C₆H₅(4-CH₃)

BM = molecular weight; LogP = logarithm of octanol/water partition coefficient; MR = molar refractivity; Torsion = bond between rotating atoms (rotatable bond); HBA = hydrogen bond acceptors; HBD = hydrogen bond donors; PSA = polar surface activity.

Table 2 ADMET properties of FA derivatives by ProTox Online Tool.

Code	Absorbtion			Distribution			Metabolism		Excretion	Toxicity			Class
	Intestinal abs.	Skin Permeability	Caco-2 permeability	VDss	BBB permeability	CNS Permeability	CYP 2D6 inhibitor	CYP 3A4 inhibitor	Total Clearance	Ames Toxicity	Hepato toxicity	LD50 (mg/kg)	
FA1	93.921	-2.881	0.279	-0.851	-0.242	-2.573	no	no	0.621	no	no	2000	4
FA2	97.322	-2.992	1.253	-0.457	-0.025	-2.493	no	no	0.636	yes	no	2980	5
FA3	96.903	-2.961	1.275	-0.392	-0.010	-2.501	no	no	0.666	yes	no	1772	4
FA4	96.483	-2.901	1.300	-0.335	-0.005	-2.497	no	no	0.679	yes	no	1772	4
FA5	96.064	-2.852	1.325	-0.276	-0.021	-2.493	no	no	0.695	no	no	1772	4
FA6	95.645	-2.814	1.415	-0.217	-0.036	-2.490	no	no	0.714	no	no	7900	6
FA7	100.00	-2.678	1.298	-0.409	-0.129	-1.671	no	no	0.721	no	no	9600	6
FA8	96.937	-2.876	0.376	-0.994	-0.366	-2.639	no	no	0.718	no	no	9600	6
FA9	96.518	-2.845	0.944	-0.942	-0.391	-2.635	no	no	0.745	yes	no	1772	4
FA10	96.099	-2.818	0.943	-0.887	-0.415	-2.631	no	no	0.762	yes	no	3450	5
FA11	95.680	-2.795	0.942	-0.829	-0.439	-2.627	no	no	0.781	no	no	1772	4
FA12	95.261	-2.776	0.942	-0.768	-0.463	-2.624	no	no	0.800	no	no	1772	4
FA13	96.301	-2.830	1.036	-1.066	-0.350	-2.293	no	no	0.655	yes	no	1772	4
FA14	94.641	-2.826	1.019	-1.099	-0.543	-2.178	no	no	0.070	no	no	3450	5
FA15	96.099	-2.831	1.041	-1.034	-0.343	-2.218	no	no	0.658	no	no	3450	5
FA16	96.298	-2.866	1.053	-1.186	-0.603	-2.914	no	no	0.610	no	no	3450	5
FA17	94.928	-2.949	1.214	-0.082	-0.007	-2.578	no	no	0.396	no	no	3450	5
FA18	94.509	-2.934	1.235	-0.018	-0.023	-2.586	no	no	0.481	no	no	3450	5
FA19	94.089	-2.906	1.260	-0.037	-0.038	-2.582	no	no	0.696	no	no	3450	5
FA20	96.601	-2.843	1.312	-0.809	0.015	-2.132	no	no	0.519	no	no	300	3
FA21	96.398	-2.846	1.333	-0.777	0.027	-2.057	no	no	0.520	no	yes	300	3
FA22	60.253	-2.979	0.228	-0.883	-0.732	-2.599	no	no	0.537	no	no	300	3
FA23	97.073	-2.931	0.421	-1.173	-0.600	-3.177	no	no	0.715	yes	no	500	4
FA24	94.109	-2.878	0.325	-0.815	-0.230	-2.689	no	no	0.321	no	no	500	4

Skin permeability is an important consideration for improving drug efficacy that is particularly of interest in the development of transdermal drug delivery. A molecule will barely penetrate the skin if log Kp is more than -2.5 cm/h [21]. From Table 2 it can be seen that the skin permeability (Kp) of ferulic acid derivatives ranges from -2.678 to -2.992 cm/h (< -2.5). Therefore, it can be predicted that all derivatives have good skin penetrability.

The Caco-2 cell line is composed of human epithelial colorectal adenocarcinoma cells. The Caco-2 monolayer of cells is widely used as an *in vitro* model of the human intestinal mucosa to predict the absorption of orally administered drugs by measuring the log of the evident permeability coefficient (log Papp; log cm/s). A compound is considered to have a high Caco-2 permeability if it has Papp > 8 x 10⁶ cm/s. For the pkCSM predictive model, high Caco-2 permeability is translated into predicted log Papp values > 0.90 cm/s [21].

From Table 2 it can be seen that the Caco-2 permeability value (log Papp) of the ferulic acid derivatives ranges from 0.228 to 1.415 cm/s, and there are 19 compounds with log Papp > 0.9 cm/s, so it can be predicted that the compounds

have a high Caco-2 permeability. Five FA derivatives, FA1, FA8, FA22, FA23, and FA24, have $\log P_{app} < 0.9$ cm/s, so it is predicted that these compounds have low Caco-2 permeability.

The volume of distribution (VD) is the calculated volume that the whole quantity of a medicine will be circulated at an equal level of blood plasma. The higher the VD is, the larger the amount of a drug is distributed to tissue rather than plasma. This model is established from the estimation of the steady-state volume of distribution (VD_{ss}), which is then revealed as $\log L/kg$. According to Pires *et al.* [21], VD_{ss} higher than 2.81 L/kg ($\log VD_{ss} > 0.45$) is categorized as high, whereas VD_{ss} lower than 0.71 L/kg ($\log VD_{ss} < -0.15$) is categorized as low [12]. From Table 3 it can be seen that the VD_{ss} values of the FA derivatives range from -1.186 to 0.037, and three compounds have a VD_{ss} value of < -0.15 , i.e. FA18, FA19, and FA20, so it can be predicted that almost all derivatives of these compounds can be distributed evenly providing an equal level of blood plasma.

The blood-brain barrier (BBB) secures the brain from exogenous compounds. The ability of a drug to cross into the brain is an important parameter to consider for reducing side effects and toxicities or to improve the efficacy of drugs whose pharmacological activity is within the brain. The permeability of the blood-brain barrier is calculated *in vivo* as $\log BB$, the logarithmic ratio of the brain-to-plasma drug concentration. Molecules are able to pass through the blood brain barrier promptly when $\log BB$ is higher than 0.3, but compounds with $\log BB$ smaller than -1 barely reach the brain [21]. From Table 2 it can be seen that the ranges of $\log BB$ value of the FA derivatives range from -0.732 to 0.129, which means greater than -1, so it can be predicted that all the derivatives are able to penetrate the blood-brain barrier moderately.

The permeability of the blood-surface area of the central nervous system (CNS) permeability ($\log PS$) is a direct measurement that can be obtained from *in situ* brain perfusions with the compound directly injected into the carotid artery. This lacks systemic distribution effects that may distort brain penetration [21]. Compounds with $\log PS > -2$ are considered to be able to penetrate the CNS, while those with $\log PS < -3$ are considered to be unable to penetrate the CNS [21]. From Table 2 it can be seen that the $\log PS$ values of the FA derivatives range from -1.671 to -3.177. There is one compound (FA7, $\log PS = -1.617$) capable of penetrating the CNS, one compound (FA23, $\log PS = -3.177$) that is unable to penetrate the CNS, while the other derivatives are able to penetrate the CNS moderately.

Cytochrome P450 is an important detoxification enzyme in the body, mainly found in the liver. It oxidizes xenobiotics to facilitate their excretion. Many

drugs are deactivated by cytochrome P450's but some can be activated by it. Inhibitors of this enzyme, such as grapefruit juice, can affect drug metabolism and are contraindicated. The cytochrome P450's are responsible for the metabolism of many drugs. However, inhibitors of the P450's can dramatically alter the pharmacokinetics of these drugs, so it is important to evaluate whether a given compound is likely to be a cytochrome P450 substrate. The two main isoforms responsible for drug metabolism are P2D6 cytochrome (CYP2D6) and P3A4 cytochrome (CYP3A4) [21]. From Table 2 it can be seen that almost all ferulic acid derivatives do not affect or inhibit the CYP2D6 and CYP3A4 enzymes, except the FA20 and FA21 compounds, which can affect the CYP3A4 enzyme, so it can be predicted that the derivatives tend to be metabolized by the P450 enzymes in the body.

Organic cation transporter 2 (OCT2) is a protein transporter that has a vital contribution in renal uptake, disposition, and clearance of drugs and endogenous compounds. OCT2 substrates have potential for adverse interactions with codirected OCT2 inhibitors. Evaluating the transfer of a candidate compound by OCT2 offers useful information regarding not only its clearance but also potential contraindications [21]. From Table 2 it can be seen that not all FA derivatives affect the OCT2 substrate, so it can be predicted that the derived compounds are not OCT2 substrates.

A steady-state level is reached when the drug is bioavailable and administered at the appropriate dosing rate. Both of these are dependent on drug clearance, which can be determined from the total of hepatic (metabolism in the liver and biliary clearance) and renal clearance (excretion via the kidneys). The higher the CLTOT value of the compound, the faster the excretion process [21]. From Table 2 it can be seen that the log CLTOT value of the ferulic acid derivatives ranges from -0.070 to 0.800 ml/min/kg and from these values the rate of excretion of the compound can be predicted.

Determining the toxicity of the compound can be done by the Ames toxicity test. The Ames test is a method to predict the mutagenic potential of a compound using bacteria. A positive test indicates that the compound is mutagenic and therefore may act as a carcinogen [21]. From Table 2 it can be seen that seven FA derivatives, FA2, FA3, FA4, F9, FA10, FA13, and FA23, are predicted to have mutagenic effects.

Another toxicity test is the hepatotoxicity test. One of the most concerning safety aspects in drug development research is drug-induced liver injury, which also increases the drug attrition rate. The compound that showed at least one pathological or physiological hepatic event was considered hepatotoxic and highly related to liver disruption. From Table 2 it can be seen that almost all of

the ferulic acid derivatives are not hepatotoxic. Only one compound (FA-21) is predicted to induce hepatotoxic effects.

The potential toxicity of a prospective compound has to be assessed. The acute toxicity and relative toxicity of different compounds can be determined from the lethal dosage value. To complement the toxicity prediction of ferulic acid derivatives there is an acute oral toxicity test for rodents (LD50) and an acute toxicity classification of compounds based on the Globally Harmonized System (GSH) using the Protox online tool. From Table 2 it can be seen that the prediction for the LD50 values of the ferulic acid derivatives range from 300 to 9600 mg/kg, which means that they are included in toxicity classes from GSH Tables 3-6, i.e. the compounds have toxicity indications ranging from 'has harmful effects when swallowed' to 'is not toxic' (Table 2).

There are three FA derivatives that belong to category 3 GSH ($LD50 = > 50 \leq 300$ mg/kg), i.e. FA20, FA21, FA22, which means that those compounds have toxic effects when swallowed, and three compounds belong to category 6 GSH ($LD50 = > 5000$ mg/kg), i.e. FA6, FA7, and FA8, which means that they are not toxic. Eight compounds belong to category 5 ($LD50 = > 2000 \leq 5000$ mg/kg), i.e. FA2, FA10, FA14-19, which means that these compounds have relatively low acute toxicity. The other nine compounds belong to category 4, which means they are slightly toxic.

3.3 Physicochemical-ADMET Properties Relationships

Based on the regression analysis performed between the *in silico* activities on the P2Y₁₂ receptor (MDS, Figure 1) with each physicochemical property, i.e. Log P, MR, and E_{total} , shown in Table 1, some linear relationships were found between the *in silico* activity on the P2Y₁₂ receptor with each of the physicochemical properties, i.e.:

$$MDS = -2.204 \text{ Log P} - 0.705 \text{ MR} - 70.134 \quad (4)$$

$$(n=24, \text{ Adjust } R^2=0.696, F=27.386, s=6.98)$$

$$MDS = -11.168 \text{ Log P} - 0.307 E_{total} - 92.263 \quad (5)$$

$$(n=24, \text{ Adjust } R^2=0.643, F=18.933, s=7.92)$$

$$MDS = -0.707 \text{ MR} - 0.331 E_{total} - 67.985 \quad (6)$$

$$(n=24, \text{ Adjust } R^2=0.735, F=32.901, s=6.52)$$

$$MDS = 0.396 \text{ Log P} - 0.725 \text{ MR} - 0.337 E_{total} - 67.506 \quad (7)$$

$$(n=24, \text{ Adjust } R^2=0.722, F=20.901, s=6.68)$$

The equation that showed the highest significance was the relationship between MDS and combined MR- E_{total} , denoted by Eq. (6) ($P < 0.05$, adjusted $R^2 = 0.735$, and $F = 32.901$). However, the coefficients of each physicochemical variable in the regression equations were negative, indicating unfavorable relationships. The addition of Log P or E_{total} in the regression equations containing molar refractivity decreased the significance (F value) and the coefficient of each physicochemical variable was still negative.

The combination of three physicochemical variables in one equation also decreased the significance (F value) but gave a positive variable coefficient for Log P. These results indicate that the physicochemical properties (Log P, MR, and E_{total}) will contribute positively to ligand-receptor interactions when combined.

4 Conclusion

From this study it was concluded that all FA derivatives have good ADMET profiles, except three derivatives that are harmful when swallowed. Compound FA19 has the greatest activity as antiplatelet agent based on its interaction with the P2Y₁₂ receptor.

Acknowledgements

This research was financially supported by DRPM DIKTI 2017.

References

- [1] Agency of Research and Development, *Research of Basic Health 2013*, Ministry of Health Republic Indonesia, pp. 1-384, 2013. <http://www.depkes.go.id/resources/download/general/Hasil/Riskesdas/2013.pdf>, (10 April 2017). (Text in Indonesian)
- [2] Ahn, Y.A, Lee, J-Y., Park H.D., Kim, T.H., Park, M.C., Choi, G. & Kim S., *Identification of a New Morpholine Scaffold as a P2Y₁₂ Receptor Antagonist*, *Molecules*, **21**(9), pp. 1114, 2016. DOI:10.3390/molecules21091114
- [3] North, R.A. & Jarvis, M.F., *P2X receptors as Drug Targets*, *Mol. Pharmacol.*, **83**(4), pp. 759-769, 2013. DOI:10.1124/mol.112.083758
- [4] Cattaneo, M., *Advances in Antiplatelet Therapy: Overview of New P2Y₁₂ Receptor Antagonists in Development*, *Eur. Hear. J. Suppl.*, **10**(Suppl I), pp. I33–I37, 2008. DOI:10.1093/eurheartj/sun037
- [5] Paoletta, S., Sabbadin, D., Kugelgen, I. von, Hinz, S., Katritch, V., Hoffmann, K., Abdelrahman, A., Strabburger, J., Baqi, Y., Zhao, Q., Stevens, R.C., Moro, S., Muller, C.E., Jacobson, K.A., *Modelling Ligand*

- Recognition at P2Y₁₂ Receptor in Ligth of X-Ray Structural Information*, J Comput Aided Mol Des, **29**(8), pp. 737-756, 2015. DOI:10.1007/s10822-015-9858-z
- [6] Dudley, A., Thomason, J., Fritz, S., Grady, J., Stokes, J., Wills, R., Pinchuk, L., Mackin, A. & Lunsford, K., *Cyclooxygenase Expression and Platelet Function in Healthy Dogs Receiving Low-Dose Aspirin*, J. Vet. Intern. Med., **27**(1), pp. 141–149, 2013. DOI:10.1111/jvim.12022
- [7] Kumalo, H.M., Bhakat, S. & Soliman, M.E., *Theory and Applications of Covalent Docking in Drug Discovery: Merits and Pitfalls*, Molecules, **20**(2), pp. 1984-2000, 2015. DOI:10.3390/molecules20021984
- [8] Chelucci, R.C., Dutra, L.A., Lopes Pires, M.E., de Melo, T.R., Bosquesi, P.L., Chung, M.C. & Dos Santos, J.L., *Antiplatelet and Antithrombotic Activities of Non-steroidal Anti-inflammatory Drugs Containing an n-Acyl Hydrazone Subunit*, Molecules, **19**(2), pp. 2089-2099, 2014. DOI:10.3390/molecules19022089
- [9] Zhang, P-X., Lin, H., Qu, C., Tang, Y-P., Li, N-G., Kai, J. Shang, G., Li, B., Zhang, L. Yan, H., Liu, P. & Jin-Ao Duan, J-A., *Design, Synthesis, and In Vitro Antiplatelet Aggregation Activities of Ferulic Acid Derivatives*, J. Chem., **2015**(Art.ID. 376527), pp. 1-7, 2015. DOI:10.1155/2015/376527
- [10] Yang, X.Z., Diao, X.J., Yang, W.H., Li, F., He, G.W., Gong, G.Q. & Xu, Y.G., *Design, Synthesis and Antithrombotic Evaluation of Novel Dabigatran Prodrugs containing Methyl Ferulate*, Bioorganic Med. Chem. Lett., **23**(7), pp. 2089–2092, 2013. DOI:10.1016/j.bmcl.2013.01.126
- [11] Li, J., Zhou, N., Luo, K., Zhang, W., Li, X., Wu, C. & Bao, J., *In Silico Discovery of Potential VEGFR-2 Inhibitors from Natural Derivatives for Anti-angiogenesis Therapy*, Int. J. Mol. Sci., **15**(9), pp. 15994-16011, 2014. DOI:10.3390/ijms150915994
- [12] Somer Jr., F.L., *Molecular Modelling for Beginners (Alan Hinchliffe)*, J. Chem. Educ., **81**(11), pp. 1573, 2004. DOI:10.1021/ed081p1573
- [13] Tsaioun, K., Blaauboer, B.J. & Hartung, T., *Evidence-based Absorption, Distribution, Metabolism, Excretion (ADME) and its Interplay with Alternative Toxicity Methods*, ALTEX, **33**(4), pp. 343-358, 2016. DOI:10.14573/altex.1610101
- [14] Moroy, G., Martiny, V.Y., Vayer, P., Villoutreix, B.O. & Miteva, M.A., *Toward in Silico Structure-based ADMET Prediction in Drug Discovery*, Drug Discov. Today, **17**(1–2), pp. 44–55, 2012. DOI: 10.1016/j.drudis.2011.10.023
- [15] Rutgers and UCSD/SDSC, *4PXZ Crystal Structure in Complex with 2MeSADP*, RCSB Protein Data Bank, <http://www.rcsb.org/structure/4pxz>, (12 December 2016). DOI: 10.2210/pdb4PXZ/pdb

- [16] National Cancer Institute, *Online SMILES Translator*, United States <https://cactus.nci.nih.gov/translate/>, (20 June 2017).
- [17] Pires, D.E.V., Blundell, T.L. & Ascher, D.B., *The University of Melbourne's pkCSM Small-molecule Pharmacokinetics Prediction*, <http://biosig.unimelb.edu.au/pkcsm/prediction/>, (20 June 2017).
- [18] Charite University of Medicine-Institute for Physiology, *ProTox-II – Prediction Of Toxicity Of Chemicals*, http://tox.charite.de/protox_II/ (20 June 2017).
- [19] Kaushik, P., Lal Khokra, S., Rana, A.C. & Kaushik, D., *Pharmacophore Modeling and Molecular Docking Studies on Pinus roxburghii as a Target for Diabetes Mellitus*, *Adv. Bioinformatics*, **2014**(Art.ID. 903246), 2014. DOI:10.1155/2014/903246
- [20] Lipinski, C.A., Lombardo, F., Dominy, B.W. & Feeney, P.J., *Experimental and Computational Approaches to Estimate Solubility and Permeability in Drug Discovery and Development Settings*, *Adv. Drug Deliv. Rev.*, **23**(1-3), pp. 3-26, 1997.
- [21] Pires, D.E., Blundell, T.L. & Ascher, D.B., *pkCSM: Predicting Small-molecule Pharmacokinetic and Toxicity Properties using Graph-based Signatures*, *J. Med. Chem.*, **58**(9) pp. 4066-4072, 2015. DOI:10.1021/acs.jmedchem.5b00104